

Effect of thermal radiation on unsteady convective heat transfer flow of a rotating nano-fluid past a vertical plate

K. Sree Ranga Vani¹ and D. R. V. Prasada Rao²

¹Department of Mathematics, Sri Sathya Sai Institute of Higher Learning, Anantapur

²Department of Mathematics, Sri Krishna Devaraya University, Anantapur

ABSTRACT

In this paper we investigate the effect of thermal radiation and oscillatory temperature on unsteady convective heat transfer flow of a nanofluid past a vertical plate in the presence of heat generating sources. Analytical closed form solutions are obtained for both the momentum and the energy equations using the regular perturbation method. Graphs are used to illustrate the significance of key parameters on the nanofluid velocity and temperature distributions.

Keywords: Thermal Radiation, Heat transfer, Nanofluid, Vertical Plate

INTRODUCTION

Nano fluid are solid-liquid composite materials consisting of solid nanoparticles or nanofibers, with sizes typically on the order of 1–100 nm, suspended in a liquid. Nano fluids are characterized by an enrichment of a base fluid like water, toluene, ethylene glycol or oil with nanoparticles in variety of types like Metals, Oxides, Carbides, Carbon, Nitrides, etc. Today nanofluid are sought to have wide range of applications in medical application, biomedical industry, detergency, power generation in nuclear reactors and more specifically in any heat removal involved industrial applications. The ongoing research ever since then has extended to utilization of nano-fluids in microelectronics, fuel cells, pharmaceutical processes, hybrid-powered engines, engine cooling, vehicle thermal management, domestic refrigerator, chillers, heat exchanger, nuclear reactor coolant, grinding, machining, space technology, defense and ships, and boiler flue gas temperature reduction [1]. Indisputably, the nano fluids are more stable and have acceptable viscosity and better wetting, spreading, and dispersion properties on a solid surface [2, 17]. Several reviews [5, 15] on nano fluids with respect to thermal and rheological properties have been reported.

Thus, nano fluids have an ample collection of potential applications in electronics, pharmaceutical processes, hybrid-powered engines, automotive and nuclear applications where enhanced heat transfer or resourceful heat dissipation is required. In view of these, Kiblinski et al. [14] suggested four possible explanations for the anomalous increase in the thermal conductivity of nano fluids. These are nanoparticles clustering, Brownian motion of the particles, molecular level layering of the liquid/particles interface and ballistic heat transfer in the nanoparticles. Despite a vast amount of literature on the flow of nanofluid model proposed by Buongiorno [4], we are referring to a few recent studies [3,6,19] in this article. However, we are following the nanofluid model proposed by Tiwari and Das [24], which is being used by many current researchers [7,8,18] on various flow fields.

The study of MHD flow and heat transfer due to the effect of a magnetic field in a rotating frame of reference has attracted the interest of many investigators in view of its applications in many industrial, astrophysical (dealing with the sunspot development, the solar cycle and the structure of a rotating magnetic stars), technological and engineering applications (MHD generators, ion propulsion, MHD pumps, etc.) and many other practical applications, such as in biomechanical problems (e.g., blood, flow in the pulmonary alveolar sheet). Many authors have studied the flow and heat transfer in a rotating system with various geometrical situations [1,10,11,16]. Hamad [9] investigated the effect of a transverse magnetic field on free convection flow of a nanofluid past a vertical semi-infinite flat plate. Recently, Satya Narayana et al. [22] studied the Hall current and radiation absorption effects on MHD micropolar fluid in a rotating system. Some other related works can also be found in recent papers [12, 13, 20, 23].

Thermal radiation is important in some applications because of the manner in which radiant emission depends on temperature and nanoparticles volume fraction. The thermal radiation effect on mixed convection heat transfer in porous media has many important applications such as the sensible heat storage bed, the nuclear reactor cooling system, space technology, and underground nuclear waste disposal. To the best of the author's knowledge (from the literature), no studies have been communicated thus far with regard to the study of flow and heat transfer distinctiveness of a nanofluid past a vertical plate with thermal radiation in a rotating frame of reference. Recently Satyanarayana et al [21] have studied the effect of radiation on the convective heat transfer flow of a rotating nanofluid past a porous vertical plate with oscillatory velocity.

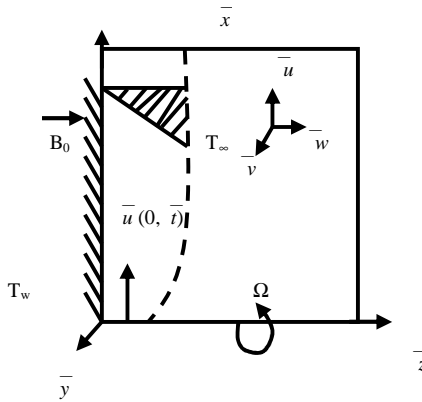
In this paper we investigate the effect of thermal radiation on unsteady convective heat transfer flow of a nanofluid past a vertical plate in the presence of heat generating sources. Analytical closed form solutions are obtained for both the momentum and the energy equations using the regular perturbation method. Graphs are used to illustrate the significance of key parameters on the nanofluid velocity and temperature distributions.

Nomenclature

B_0 : constant applied magnetic field
 C_f : skin friction coefficient
 E : applied electric field
 F : heat radiation parameter
 g : acceleration due to gravity
 K : permeability parameter
 k : permeability of porous medium
 k : mean absorption coefficient
 M : dimensionless magnetic field parameter
 Nu : local Nusselt number
 Nur : reduced Nusselt number
 Pr : Prandtl number
 Q : dimensional heat source parameter
 Q_H : dimensional heat source
 q_r : radiative heat flux
 q_w : heat flux from the plate
 R : dimensional rotational parameter
 Re_x : local Reynolds number
 S : suction parameter
 T : local temperature of the nanofluid
 T_w : wall temperature of the fluid
 T_∞ : temperature of the ambient nanofluid
 U_0 : characteristic velocity
 w_0 : normal velocity
 (x, y, z) : Cartesian coordinates

Greek Symbols

α : thermal diffusivity
 α_f : thermal diffusivity of the fluid
 α_{nf} : thermal diffusivity of the nanofluid
 β : thermal expansion coefficient
 β_f : coefficient of thermal expansion of the fluid
 β_s : coefficient of thermal expansion of the solid
 ρ_f : density of the fluid friction
 ρ_s : density of the solid friction
 ρ_{nf} : density of the nanofluid
 η : kinematic viscosity
 η_f : kinematic viscosity of the fluid
 μ : dynamic viscosity
 μ_{nf} : viscosity of the nanofluid
 σ : electrical conductivity of the fluid
 σ^* : Stefan–Boltzmann constant parameter
 $(\rho C)_{nf}$: heat capacitance of the nanofluid
 ϵ : small constant quantity
 χ : complex function
 θ : non-dimensional temperature
Subscripts
 f : fluid, s : solid, nf : nanofluid
 w : condition at the wall,
 ∞ : condition at free stream
 (u, v, w) : velocity components along x and y axes



FORMULATION OF THE PROBLEM

We analyze a transient, three dimensional flow of a nanofluid consisting of a base fluid and small nanoparticles over a semi-infinite porous vertical plate with thermal radiation. A uniform magnetic field of strength H_0 is applied normal to the plate. It is assumed that there is no applied voltage which implies the absence of an electric field. The flow is assumed to be in the x-direction which is taken along the plane in an upward direction and z-axis is normal to the plate. Also it is assumed that the whole system is rotating with a constant angular velocity vector $\bar{\Omega}$ about the z-axis. The fluid is assumed to be gray, absorbing emitting but not scattering medium. The radiative heat flux in the x-direction is considered negligible in comparison with that in the z-direction. Due to a semi-infinite plate surface assumption, the flow variables are functions of z and t only. Figure.1 shows the problem under consideration and the co-ordinate system. In the present problem, the following assumptions have been made:

The plate has an oscillatory movement on time t and frequency n with velocity $u(0,t)$, which is given by $\bar{u}(0,t) = U_0(1 + \varepsilon \cos(\bar{n}, \bar{t}))$. Initially $\bar{t} < 0$ the fluids as well as the plate are at rest but for $t \geq 0$ the whole system is allowed to rotate with a constant velocity Ω about the z-axis. It is assumed that the there is no applied voltage which implies that an electric field is absent. In a physically realistic situation, we cannot ensure perfect insulation in any experimental set-up. There will always be some fluctuations in the temperature. The plate temperature is assumed to vary harmonically with time. It varies from $T_w^* + \varepsilon(T_w^* - T_\infty^*)$ as t varies from 0 to $2\pi/\omega$. Since ε is small, the plate temperature varies only slightly from the mean value T_w^* . The ambient temperature has the constant value T_∞ . The conservation equation of current density $\nabla \cdot \bar{J} = 0$ gives $J_z = \text{constant}$. Under the above mentioned assumptions, the equation of momentum and thermal energy respectively, can be written in dimensional form as :

$$\frac{\partial w}{\partial z} = 0 \quad (1)$$

$$\frac{\partial u}{\partial t} + w \frac{\partial u}{\partial z} - 2\Omega v = \frac{1}{\rho_{nf}} (\mu_{nf} \frac{\partial^2 u}{\partial z^2} + (\rho \beta_{nf}) g (T - T_\infty) - (\sigma_{nf} \mu_e^2 H_0^2) u) \quad (2)$$

$$\frac{\partial v}{\partial t} + w \frac{\partial v}{\partial z} + 2\Omega u = \frac{1}{\rho_{nf}} (\mu_{nf} \frac{\partial^2 v}{\partial z^2} - (\sigma_{nf} \mu_e^2 H_0^2) v) \quad (3)$$

$$\frac{\partial T}{\partial t} + w \frac{\partial T}{\partial z} = k_{nf} \frac{\partial^2 T}{\partial z^2} - \frac{1}{(\rho C_P)_{nf}} \frac{\partial (q_r)}{\partial z} - \frac{Q_H}{(\rho C_P)_{nf}} (T - T_\infty) \quad (4)$$

The boundary conditions are:

$$u(z, t) = 0, v(z, t) = 0, T = T_w \quad \text{for } f \leq 0, \text{ and any } z$$

$$u(0, t) = U_0 (1 + \frac{\epsilon}{2} (e^{i\omega t} + e^{-i\omega t})), v(0, t) = 0, T(0, t) = T_w + (T_w - T_\infty) (e^{i\omega t} + e^{-i\omega t}) \quad (5)$$

$$u(\infty, t) \rightarrow 0, v(\infty, t) \rightarrow 0, T(\infty, t) \rightarrow T_\infty \quad \text{for } t \geq 0$$

The properties of the Nano fluids are defined as follows

$$\begin{aligned} \mu_{nf} &= \mu_f / (1 - \phi)^{2.5} & \alpha_{nf} &= \frac{k_{nf}}{(\rho C_p)_{nf}} & \rho_{nf} &= (1 - \phi) \rho_f + \phi \rho_s \\ (\rho C_p)_{nf} &= (1 - \phi) (\rho C_p)_f + \phi (\rho C_p)_s & (\rho \beta)_{nf} &= (1 - \phi) (\rho \beta)_f + \phi (\rho \beta)_s \\ k_{nf} &= \frac{k_f (k_s + 2k_f - 2\phi(k_f - k_s))}{(k_s + 2k_f + 2\phi(k_f - k_s))}, \sigma_{nf} = \sigma_f \left[1 + \frac{3(\sigma - 1)\phi}{(\sigma + 2) - (\sigma - 1)\phi} \right], \sigma &= \frac{\sigma_s}{\sigma_f} \end{aligned} \quad (6)$$

$$\text{We consider the solution of equation (1) as } w = -w_0 \quad (7)$$

The radiation heat term by using The Roseland approximation is given by

$$q_r = -\frac{4\sigma^*}{3\beta_R} \frac{\partial T'^4}{\partial z}, T'^4 \cong 4TT_\infty^3 - 3T_\infty^4, \quad \frac{\partial q_R}{\partial z} = -\frac{16\sigma^* T_\infty^3}{3\beta_R} \frac{\partial^2 T}{\partial z^2} \quad (8)$$

We introduce the following dimensionless variables:

$$\begin{aligned} z' &= \frac{U_0}{v_f} z, & t' &= \frac{U_0^2}{v_f} t, & n' &= \frac{v_f}{U_0^2} n, & u' &= \frac{u}{U_0}, & v' &= \frac{v}{U_0} & \theta &= \frac{T - T_\infty}{T_w - T_\infty} \\ S &= \frac{w_0}{U_0} & M &= \frac{\sigma_f \mu e H_0^2 v_f}{\rho_f U_0^2} & R &= \frac{2\Omega v_f}{U_0^2} & Q &= \frac{Q_H v_f^2}{k_f U_0^2} & F &= \frac{4\sigma^* T_\infty^3}{\beta_R k_f} \end{aligned} \quad (9)$$

Equations(2)-(4) in the non-dimensional form are

$$\frac{\partial u}{\partial t} - S \frac{\partial u}{\partial z} - Rv = \frac{1}{A_1 A_3} \frac{\partial^2 u}{\partial z^2} + \frac{A_4}{A_3} \theta - \frac{(M^2 A_6)}{A_3} u \quad (10)$$

$$\frac{\partial v}{\partial t} - S \frac{\partial v}{\partial z} + Ru = \frac{1}{A_1 A_3} \frac{\partial^2 v}{\partial z^2} - \frac{(M^2 A_6)}{A_3} v \quad (11)$$

$$\frac{\partial \theta}{\partial t} - S \frac{\partial \theta}{\partial z} - Rv = \frac{1}{P_r} \left(\frac{A_2}{A_5} \frac{\partial^2 \theta}{\partial z^2} - \frac{1}{A_5} Q\theta \right) \quad (12)$$

Where

$$\begin{aligned} A_1 &= (1 - \phi)^{2.5} & A_2 &= \frac{k_{nf}}{k_f} + \frac{4F}{3} & A_3 &= 1 - \phi + \phi \left(\frac{\rho_s}{\rho_f} \right) \\ A_4 &= 1 - \phi + \phi \left(\frac{(\rho \beta)_s}{(\rho \beta)_f} \right) & A_5 &= 1 - \phi + \phi \frac{(\rho C_p)_s}{(\rho C_p)_f}, A_6 &= 1 + \frac{3(\sigma - 1)\phi}{(\sigma + 2) - (\sigma - 1)\phi} \end{aligned}$$

The boundary conditions (5) reduce to

$$\begin{aligned} u(z, t) &= 0 & v(z, t) &= 0 & \theta(z, t) &= 0 \quad \text{for } t \leq 0 \quad \text{and any } z \\ u(0, t) &= 1 + \frac{\epsilon}{2} (e^{iwt} + e^{-iwt}), v(0, t) = 0 & \theta(0, t) &= 1 + \frac{\epsilon}{2} (e^{iwt} + e^{-iwt}) \\ u(\infty, t) &\rightarrow 0, & v(\infty, t) &\rightarrow 0, & \theta(\infty, t) &\rightarrow 0 \quad \text{for } t \geq 0 \end{aligned} \quad (13)$$

In view of the fluid velocity in the component form: $V(z, t) = u(z, t) + iv(z, t)$

The equations (12) and (13) reduce to

$$\frac{\partial V}{\partial t} - S \frac{\partial V}{\partial z} + iRV = \frac{1}{A_1 A_3} \frac{\partial^2 v}{\partial z^2} + \frac{A_4}{A_3} \theta - \frac{M^2 A_6}{A_2} V \quad (14)$$

The boundary conditions (13) reduce to

$$\begin{aligned} V(z, t) &= 0 & \theta(z, t) &= 0 \quad \text{for } t \leq 0 \quad \text{any } z \\ V(0, t) &= 1 + \frac{\epsilon}{2} (e^{iwt} + e^{-iwt}) & \theta(0, t) &= 1 + \frac{\epsilon}{2} (e^{iwt} + e^{-iwt}) \\ V(z, t) &\rightarrow 0, & \theta(z, t) &\rightarrow 0 \quad \text{for } t \geq 0 & \text{as } z \rightarrow \infty \end{aligned} \quad (15)$$

METHOD OF SOLUTION

Equations (12) and (14) are coupled, non-linear partial differential equations and these can not be solved in closed form. However, these equations can be reduced to a set of ordinary differential equations, which can be solved analytically. This can be done representing the velocity and temperature of the fluid in the neighborhood of the plate as:

$$V(z, t) = V_0(Z, T) + \frac{\epsilon}{2} (e^{iwt} V_1(z) + e^{-iwt} V_2(z)) \quad (16)$$

$$\theta(z, t) = \theta_0(z, t) + \frac{\epsilon}{2} (e^{iwt} \theta_1(z) + e^{-iwt} \theta_2(z)) \quad (17)$$

Substituting the above expansions (16) & (17) in equations (12) and (14) and equating the harmonic and non-harmonic terms and neglecting the higher order terms of $O(\epsilon^2)$. We obtain the following set of equations:

ZEROTH ORDER EQUATIONS

$$\frac{d^2 V_0}{dz^2} + A_3 S \frac{dV_0}{dz} - A_1 (iRA_3 + M^2 A_6) V_0 + A_1 A_4 \theta_0 = 0 \quad (18)$$

$$A_2 \frac{d^2 \theta_0}{dz^2} + A_5 S \Pr \frac{d\theta_0}{dz} - Q \theta_0 = 0 \quad (19)$$

FIRST ORDER EQUATIONS:

$$\frac{d^2 V_1}{dz^2} + A_3 S \frac{dV_1}{dz} - A_1 (i(R + \omega) A_3 + M^2 A_6) V_1 + A_1 A_4 \theta_1 = 0 \quad (20)$$

$$A_2 \frac{d^2 \theta_1}{dz^2} + A_5 S \Pr \frac{d\theta_1}{dz} - (i\omega \Pr A_5 + Q) \theta_1 = 0 \quad (21)$$

SECOND ORDER EQUATIONS

$$\frac{d^2 V_2}{dz^2} + A_3 S \frac{dV_2}{dz} - A_1 (i(R - \omega) A_3 + M^2 A_6) V_2 + A_1 A_4 \theta_2 = 0 \quad (22)$$

$$A_2 \frac{d^2 \theta_2}{dz^2} + A_5 S \operatorname{Pr} \frac{d\theta_2}{dz} - (i\omega \operatorname{Pr} A_5 - Q) \theta_2 = 0 \quad (23)$$

The corresponding transformed boundary conditions are

$$\begin{aligned} V_0 &= 1, \theta_0 = 1, V_1 = 1, \theta_1 = 1, V_2 = 1, \theta_2 = 1 \quad \text{at } z = 0 \\ V_0 &\rightarrow 0, \theta_0 \rightarrow 0, V_1 \rightarrow 0, \theta_1 \rightarrow 0, V_2 \rightarrow 0, \theta_2 \rightarrow 0 \quad \text{at } z \rightarrow \infty \end{aligned} \quad (24)$$

Solving equations (19)-(23) with the boundary conditions (24) we obtain the expressions for the velocity and temperature as:

$$V(z) = V_o(z) + \frac{\epsilon}{2} (V_1(z) \exp(i\omega z) + V_2(z) \exp(-i\omega z))$$

$$\theta(z) = \theta_o(z) + \frac{\epsilon}{2} (\theta_1(z) \exp(i\omega z) + \theta_2(z) \exp(-i\omega z))$$

where

$$V_0(z) = B_1 \exp(-m_1 z) + (1 - B_1) \exp(-m_2 z), \quad V_1(z) = B_2 \exp(-m_3 z) + (1 - B_2) \exp(-m_4 z)$$

$$V_2(z) = B_3 \exp(-m_5 z) + (1 - B_3) \exp(-m_6 z), \quad \theta_0(z) = \exp(-m_1 z), \quad \theta_1(z) = \exp(-m_3 z), \quad \theta_2(z) = \exp(-m_5 z)$$

The physical quantities of interest are skin friction and Nusselt number which are respectively, defined as:

$$C_f = \frac{\tau_w}{\rho_f U_o^2}, \quad Nu = \frac{xq_w}{k_f (T_w - T_\infty)}$$

Where τ_w and q_w are the wall shear and the wall heat flux from the plate respectively, which are given by

$$\tau_w = \mu_{nf} \left(\frac{\partial u}{\partial z} \right)_{z=0} \quad \text{and} \quad q_w = -k_{nf} \left(\frac{\partial T}{\partial z} \right)_{z=0}$$

$$C_f = \frac{1}{(1 - \phi)^{2.5}} V'(0) = -\frac{1}{A_1} ((B_1 - 1)m_2 - B_1 m_1 + \frac{\epsilon}{2} ((B_2 - 1)m_4 - B_2 m_3) \exp(i\omega z) + ((B_3 - 1)m_6 - B_3 m_5) \exp(-i\omega z))$$

$$Nu = -\frac{k_{nf}}{k_f} \theta'(0) = \frac{k_{nf}}{k_f} (m_1 + \frac{\epsilon}{2} (m_3 \exp(i\omega z) + m_5 \exp(-i\omega z)))$$

Where

$$m_1 = \frac{A_5 S \operatorname{Pr} + \sqrt{(A_5 S \operatorname{Pr})^2 + 4A_2 Q}}{2A_2}, \quad \beta_1^2 = iR A_3 + M^2 A_6$$

$$m_2 = \frac{A_3 S + \sqrt{(A_3 S)^2 + 4\beta_1^2}}{2}, \quad \beta_2^2 = i\omega \operatorname{Pr} A_5$$

$$m_3 = \frac{A_5 S \operatorname{Pr} + \sqrt{(A_5 S \operatorname{Pr})^2 + 4A_2 \beta_2^2}}{2A_2}, \quad \beta_3^2 = i(R + \omega) A_3 + M^2 A_6$$

$$\begin{aligned}
 m_4 &= \frac{A_3 S + \sqrt{(A_3 S)^2 + 4\beta_3^2}}{2}, & \beta_4^2 &= i\omega \operatorname{Pr} A_5 \\
 m_5 &= \frac{A_5 S \operatorname{Pr} + \sqrt{(A_5 S \operatorname{Pr})^2 + 4A_2 \beta_4^2}}{2A_2}, & \beta_5^2 &= i(R - \omega)A_3 + M^2 A_6 \\
 m_6 &= \frac{A_3 S + \sqrt{(A_3 S)^2 + 4\beta_5^2}}{2}, & B_1 &= -\frac{A_2 A_4}{m_1^2 - m_1 A_3 S - \beta_1^2} \\
 B_2 &= -\frac{A_1 A_4}{m_3^2 - m_3 A_3 S - \beta_3^2}, & B_3 &= -\frac{A_1 A_4}{m_5^2 - m_5 A_3 S - \beta_5^2}
 \end{aligned}$$

RESULTS AND DISCUSSION

A mathematical assessment for the analytical solution of this problem is performed, and the outcomes are illustrated graphically in Figures 1- 8. They explain the fascinating features of important parameters on the nanofluid velocity, temperature, skin friction and Nusselt number distributions in a rotating system for three different types of water based nano fluids. We take the values of the nanofluid volume fraction ϕ in the range of $0 \leq \phi \leq 0.08$. However, Muthtamilselvan have considered for the convective flow in a lid driven cavity, the value of the nanofluid volume fraction in the range $0 \leq \phi \leq 0.08$. If the concentration exceeds the maximum level of 0.08, sedimentation could take place. We have chosen here $n = 10$, $nt = \pi/2$, $\varepsilon = 0.02$, $\operatorname{Pr} = 6.2$ while M , R , S , ϕ , Q , F are varied over a range, which are listed in the figure legends. Fig.1 represents the effect of magnetic field on the nanofluid velocity profile. It is found that the nanofluid velocity field reduces with increase of magnetic field parameter M along the surface. These effects are much significant near the surface of the plate. This shows that the fluid velocity is reduced by increasing the magnetic field and confirms the fact that the application of the magnetic field to an electrically conducting fluid produces a dragline force which causes a retardation in the fluid velocity. We also find that the nano fluid velocity in the case of CuO_2 – water nanofluid is relatively greater than that of Al_2O_3 -water nanofluid. This phenomenon has good agreement with the physical realities. Fig.2 represents the nanofluid velocity profiles for different values of rotational parameter R . This result displays that the nanofluid velocity reduces with an increase in R , as noted in reference [14]. Further, we find that the Al_2O_3 -water nanofluid exhibits lower velocity than the flow as compared to the Cu-water nanofluid. Figs.3 & 8 shows that the nanofluid velocity and temperature with suction parameter S in the case of Cu and Al_2O_3 nanoparticles respectively. It can be seen from the profiles of nanofluid velocity that it reduces for higher S which indicates that the suction stabilizes the boundary growth. The free convection effect is also apparent in this figure. For a fixed S , the nanofluid velocity is found to increase and reaches a maximum value in a region close to the leading edge of the plate, and then gradually decreases to zero. The effect of S on the nanofluid velocity is the reverse in the case of Hamad et al [14]. This is due to the dominate role of the radiation in the fluid field. These results are clearly supported from the physical point of view. We also notice that Al_2O_3 -water nanofluid has lesser velocity profiles than the Cu-water nanofluid. A similar behaviour is noticed in the case of temperature profiles except that the temperature profile for Aluminium-water nanofluid is relatively higher than that of copper-water nanofluid. Figs.4 & 9 represents the behaviour of nanofluid velocity and temperature for different values of heat generation parameter Q_1 . These figures clearly show a decreasing tendency in the velocity and temperature with an increase in Q_1 . This is due to the fact that when heat is absorbed, the buoyancy forces decreases which retards the flow rate and there by gives rise to a decrease in the velocity and temperature profiles. Figs.5 & 10 represents the variations of nanofluid velocity and temperature with different values of Prandtl number. It is found that an increase in the Prandtl number reduces the velocity and enhances the temperature in the flow field in the case of Cu-water nanofluid while in the case of Al_2O_3 – water nanofluid, an increase in Pr enhances the velocity and reduces the temperature. Also Al_2O_3 -water exhibits relatively lower values in comparison to Cu-water nanofluid. Figs.6 & 11 displays the effect of nanoparticle volume fraction ϕ on the nanofluid velocity and temperature profiles respectively. It is found that as the nanoparticle volume fraction increases, the nanofluid velocity and temperature increase. These figures illustrate this agreement with the physical behaviour. When the volume of the nanoparticle increases, the thermal conductivity and the thermal boundary layer thickness increase. We also notice that the nanofluid velocity in the case of Al_2O_3 – water nanofluid is relatively lower than that of Cu-water nanofluid. Figs.7 & 12 exhibits the nanofluid velocity and temperature for various values of radiation

parameter F. An increase in F leads to an enhancement in the velocity and temperature distributions across the boundary layer. The effect of thermal radiation is to enhance heat transfer because of the fact that thermal boundary layer thickness increases with an increase in the thermal radiation. Thus it is pointed out that the radiation should be minimized to have the cooling process proceed at a faster rate. We also find that nanofluid velocity and temperature in the case of Al_2O_3 -water nanofluid is comparatively less than that of Cu-water nanofluid. This occurrence has a superior agreement with the physical relatives.

Table.3 displays the behaviour of local skin friction components τ_x and τ_y and Nusselt number Nu at the plate $y=0$. It is found that an increase in the Hartmann number M reduces τ_x and τ_y while an increase in the rotation parameter R reduces τ_x and enhances τ_y at $y=0$. Also τ_x and τ_y enhances with increase in the suction parameter S and the radiation parameter F and reduces with increase in the strength of the heat generating source Q for Cu-water and Al_2O_3 -water nanofluids. An increase in the nanoparticle volume fraction ϕ enhances τ_x and τ_y for Cu-water nanofluid and reduces for Al_2O_3 -water nanofluid.

The local Nusselt number (Nu) at $y=0$ is found to enhance with increase in S or Q for both Cu-water and Al_2O_3 -water nanofluids. An increase in F or ϕ enhances $|\text{Nu}|$ at $y=0$ for Cu-water nanofluid and reduces in the case of Al_2O_3 -water nanofluids. Skin friction and Nusselt number at $y=0$.

Table 1 : Thermo-physical properties of water and nanoparticles

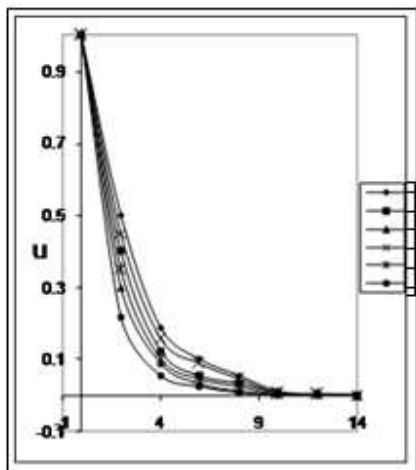
Physical properties	Water/base fluid	Cu (Copper)	Al_2O_3 (Alumina)	TiO_2 (Tin)
C_p (J/kg K)	4179	385	765	4250
ρ (kg/m ³)	997.1	8933	3970	686.2
K (W/m K)	0.613	400	40	8.9538
σ (s/m)	5.5×10^{-6}	59.5×10^6	35×10^6	2.6×10^{-6}
ϕ	0.0	0.05	0.15	0.2
$\beta \times 10^5$ (1/K)	21	1.67	0.85	0.90

Table 2 : Comparison of skin friction and Nusselt number of the present case with those of Hamad et al [8]

Pr	Skin Friction			Nusselt Number		
	$\varepsilon=0.02, F=1.0, R=0.02, n=10.0, t=0.1, M=0.5, Q=10.0, \phi=0.15, S=1.0$			$S=1.0, F=0.1, Q=10.0, \phi=0.15$		
	Present	Satyanarayana et al [21]	Hamad et al [8]	Present	Satyanarayana et al [21]	Hamad et al [8]
0.5	2.3101	2.3159708	2.3202	5.9642	5.9674231	5.9674
1.0	2.2581	2.2567503	2.2586	6.0459	6.0461932	6.0461
1.5	2.1969	2.1972895	2.1967	6.1255	6.1259433	6.1259
2.0	2.1371	2.1376083	2.1345	6.2059	6.2066709	6.2066

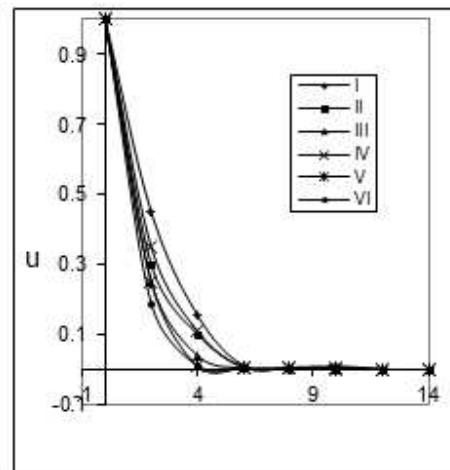
Table 3

	CuO ₂			Al ₂ O ₃		
	$\tau_x(0)$	$\tau_y(0)$	Nu(0)	$\tau_x(0)$	$\tau_y(0)$	Nu(0)
M	933.1345	458.308	-----	68.997	18.559	-----
	655.8334	122.661		48.459	5.774	
	465.2812	48.227		35.393	2.915	
S	933.1345	458.308	80.548	68.997	18.559	25.6206
	1128.780	657.097	81.779	76.928	21.776	26.8640
	1366.766	851.611	83.028	84.361	23.577	28.1631
R	933.1345	458.308	-----	68.997	18.559	-----
	591.078	464.564		53.589	25.202	
	428.805	563.276		42.225	25.448	
Q	933.1345	458.308	80.548	68.997	18.559	25.6206
	904.3385	423.895	78.748	63.001	15.541	31.3589
	880.888	397.698	64.095	58.665	13.568	36.1977
F	933.1345	458.308	80.548	68.997	18.559	25.5206
	936.797	460.289	80.388	72.084	18.533	25.1580
	942.905	463.591	79.664	77.267	18.184	24.4396
ϕ	933.1345	458.308	80.548	68.997	18.559	25.6206
	947.9516	676.085	80.551	65.633	16.2077	25.6097
	1234.443	838.125	80.553	63.502	12.4459	25.5991
	2526.783	1056.678	98.7611	59.688	10.9213	25.5885

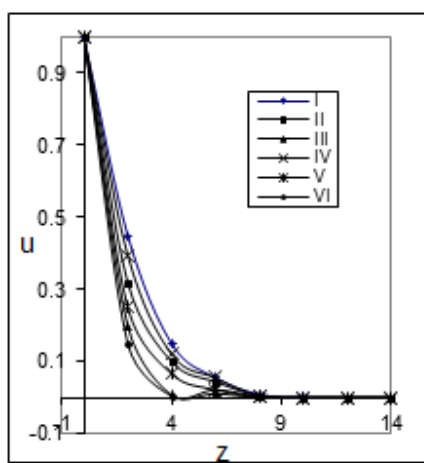
Fig.1 Variation of u with M

	I	II	III	IV	V	VI
CuO_2	0.2	1	1.5	0.2	1	1.5
Al_2O_3						

M 0.2 1 1.5 0.2 1 1.5

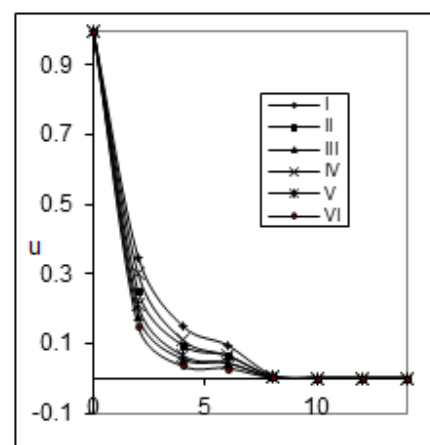
Fig.2 Variation of u with R

	I	II	III	IV	V	VI
CuO_2	0.02	0.04	0.08	0.02	0.04	0.08
Al_2O_3						

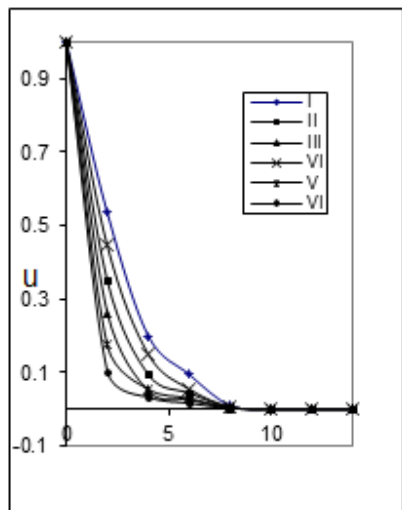
Fig.3 Variation of u with S

	I	II	III	IV	V	VI
CuO_2	0.1	0.2	0.4	0.1	0.2	0.4
Al_2O_3						

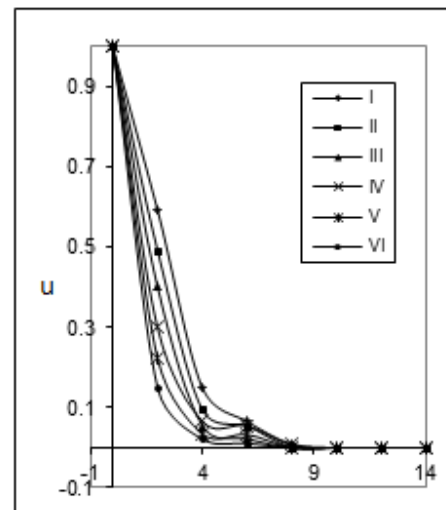
S 0.1 0.2 0.4 0.1 0.2 0.4

Fig.4 Variation of u with Q_1

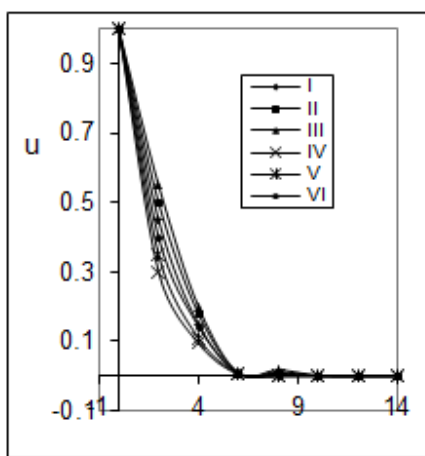
	I	II	III	IV	V	VI
CuO_2	2	4	6	2	4	6
Al_2O_3						

Fig.5 Variation of u with Pr

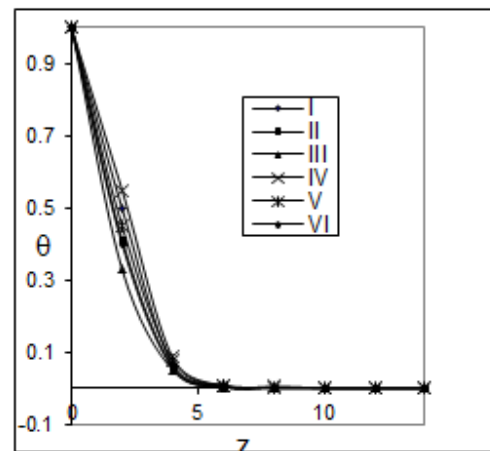
I	II	III	IV	V	VI	
CuO_2	Al_2O_3					
Pr	1	2	3	1	2	3

Fig.6 Variation of u with ϕ

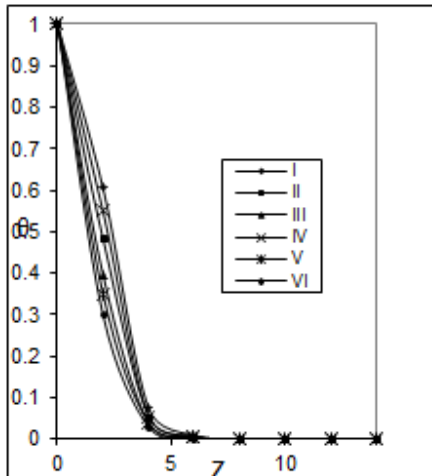
I	II	III	IV	V	VI	
CuO_2	Al_2O_3					
ϕ	0.05	0.08	0.1	0.05	0.08	0.1

Fig.7 Variation of u with F

I	II	III	IV	V	VI	
CuO_2	Al_2O_3					
F	0.2	0.4	0.8	0.2	0.4	0.8

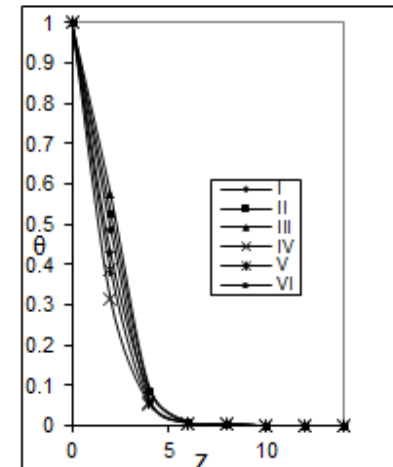
Fig.8 Variation of θ with S

I	II	III	IV	V	VI	
CuO_2	Al_2O_3					
S	0.1	0.2	0.4	0.1	0.2	0.4

Fig.9 Variation of θ with Q_1

I	II	III	IV	V	VI
CuO_2	Al_2O_3	Al_2O_3	Al_2O_3	Al_2O_3	Al_2O_3

Q1 1 2 4 6 2 4 6

Fig.10 Variation of θ with Pr

I	II	III	IV	V	VI
CuO_2	Al_2O_3	Al_2O_3	Al_2O_3	Al_2O_3	Al_2O_3

Pr 0.71 2 6.2 0.71 2 6.2

CONCLUSION

- The nanofluid velocity reduces for higher S which indicates that the suction stabilizes the boundary growth. We also notice that Al_2O_3 -water nanofluid has lesser velocity profiles than the Cu-water nanofluid. A similar behaviour is noticed in the case of temperature profiles except that the temperature profile for Aluminium-water nanofluid is relatively higher than that of copper-water nanofluid.
- There is a decreasing tendency in the velocity and temperature with an increase in heat generation parameter Q_1 .
- An increase in the Prandtl number reduces the velocity and enhances the temperature in the flow field in the case of Cu-water nanofluid while in the case of Al_2O_3 -water nanofluid, an increase in Pr enhances the velocity and reduces the temperature.
- As the nanoparticle volume fraction ϕ increases, the nanofluid velocity and temperature increase.
- An increase in the radiation parameter F leads to an enhancement in the nanofluid velocity and temperature distributions across the boundary layer.

REFERENCES

- [1]. S. Agarwal, B.S. Bhaduri, P.G. Siddheshwar, **2011**, *STRPM*, 2, 53–64.
- [2]. A. Akbarinia, M. Abdolzadeh, R. Laur, **2011**, *Applied Thermal Engineering*, 31, 556–565.
- [3]. Alsaedi, M. Awais, T. Hayat, **2012**, *Comm. Nonlinear Sci. Number Simulation*, 17, 4210–4223.
- [4]. J. Buongiorno, **2006**, *ASME J Heat Tran*, 128, 240–250.
- [5]. A. Ghadimi, R. Saidur, H.S.C. Metselaar, **2011**, *Int. J Heat Mass Tran*. 54(17-18), 4051–4068.
- [6]. M. Hajipour, A.M. Dekhordi, **2012**, *Int. J Therm. Sci.*, 55, 103–113.
- [7]. M.A.A. Hamad, M. Ferdows, **2012**, *Appl Math Mech Eng Ed*, 33(7), 923–930.
- [8]. M.A.A. Hamad, I. Pop, **2011**, *Heat Mass Tran*. 47, 1517–1524.
- [9]. M.A.A. Hamad, **2011**, *Int. Comm. Heat Mass Tran*, 38, 487–492.
- [10]. K.C.D. Hickman, **1957**, *Ind Eng Chem*, 49, 786–800.
- [11]. HideR, P.H. Robert, **1960**, *Rev Mod Phys*, 32, 799–806.
- [12]. P.K. Kameswaran, M. Narayana, P. Sibanda, P.V.S.N. Murthy, **2012**, *Int. J Heat Mass Tran*. 55, 7587–7595.
- [13]. D.Ch. Kesavaiah, P.V. Satya Narayana, S. Venkataramana, **2011**, *Int. J Appl. Math. Mech.* 7(1), 52–69.
- [14]. P. Kiblinski, S.R. Phillpot, S.U.S. Choi, J.A. Eastman, **2002**, *Int. J. Heat Mass Tran*, vol. 42, 855–863.
- [15]. I.M. Mahbubul, R. Saidur, M.A. Amalina, **2012**, *Int. J Heat Mass Tran*, 55(4), 874–885.
- [16]. B.S. Mazumder, **1991**, *ASME J Appl Mech*, 58(4), 1104–1107.
- [17]. C.T. Nguyen, G. Roy, C. Gauthier, N. Galanis, **2007**, *Appl. Thermo Eng*, 27, 1501–1506.
- [18]. B. Norifiah, I. Anuar, P. Ioan, **2012**, *Acta Mech Sin*, 28(1), 34–40.

- [19].P. Rana, R.Bhargava, **2012**, *Comm. Nonlinear Sci. Number Simulation*,7, 212–226.
- [20] .B. Rushi Kumar, R.Sivaraj, **2013**, *Int. J of Heat Mass Tran*, 56(1–2), 370– 379.
- [21].P.V.Satyanarayana, B.Venkateswarlu and S.Venkataramana,**2014**,*Heat transfer-Asian Research* DOI:10.1002/htj.211001.
- [22].P.V. Satyanarayana, B.Venkateswarlu, S.Venkataramana, **2013**, *Ain-Shams Engineering Journal*, <http://dx.doi.org/10.1016/j.asej.2013.02.002>.
- [23]. S. Srinivas, A.Subramanyam Reddy, T.R. Ramamohan, **2012**, *Int. J Heat Mass Tran*, 55, 3008– 3020.
- [24]. R.K.Tiwari, M.K.Das,**2007**, *Int. J Heat Mass Tran*, 50:2002–2018.